

ARTICLE

Role of Reduced Defects for Coupling Reactions of Acetaldehyde on Anatase $\text{TiO}_2(001)-(1\times 4)$ Surface

Yuan-yuan Ji, Yi Zheng, Xiao-chuan Ma, Xue-feng Cui*, Bing Wang*

Hefei National Laboratory for Physical Sciences at the Microscale, University of Science and Technology of China, Hefei 230026, China

(Dated: Received on January 28, 2019; Accepted on February 26, 2019)

The chemistry of acetaldehyde (CH_3CHO) adsorbed on the anatase $\text{TiO}_2(001)-(1\times 4)$ surface has been investigated by temperature-programmed desorption (TPD) method. Our experimental results provide the direct evidence that the perfect lattice sites on the anatase $\text{TiO}_2(001)-(1\times 4)$ surface are quite inert for the reaction of CH_3CHO , but the reduced defect sites on the surface are active for the thermally driven reductive carbon-carbon coupling reactions of CH_3CHO to produce 2-butanone and butene. We propose that the coupling reactions of CH_3CHO on the anatase $\text{TiO}_2(001)-(1\times 4)$ surface should undergo through the adsorption of paired CH_3CHO molecules at the reduced defect sites, since the existing reduced Ti pairs provide the suitable adsorption sites.

Key words: Acetaldehyde, Coupling reaction, Reduced defect, Anatase $\text{TiO}_2(001)$, Temperature-programmed desorption

I. INTRODUCTION

A carbon-carbon (C–C) coupling reaction is an important process for the conversion of biomass molecules to value-added chemicals [1–4], which commonly involves the key reaction step through the intermediate aldehydes [2]. As an important oxide support for metal catalysts [5], TiO_2 itself is a competent candidate (photo)catalyst for the C–C coupling reactions [6–10]. The C–C coupling reactions of aldehydes on TiO_2 have attracted wide study interests both experimentally and theoretically [11–24]. On both of the rutile TiO_2 and anatase TiO_2 surfaces, it is found that the existing surface defects are important for the C–C coupling reactions of acetaldehyde (CH_3CHO), which are consistent with the results for the reactions of other species at the defects [11, 25–34]. On the rutile $\text{TiO}_2(110)$ surface [11, 15, 23] and the rutile $\text{TiO}_2(001)$ surface [12–14], the C–C coupling reactions of CH_3CHO were observed. However, the reactions of CH_3CHO on anatase TiO_2 are seldom studied, and the roles of the defects on the reactions are less known at the atomic scale. The atomic geometries of the defects on the anatase $\text{TiO}_2(001)-(1\times 4)$ surface were identified very recently [34], that is, the “ TiO_2 ” vacancy, reduced Ti-rich defect, and partially oxidized Ti pairs in the ridges of the (1×4) reconstructed surface [26, 29, 30, 35].

In this work, we investigate the thermally

driven reductive coupling reactions of CH_3CHO on anatase $\text{TiO}_2(001)-(1\times 4)$ surface, using temperature-programmed desorption (TPD) method. The main product is 2-butanone, and the byproduct of butene is also observed. On the basis of the geometries of the identified defects, we can propose the C–C reaction route of CH_3CHO at the reduced defect sites of anatase $\text{TiO}_2(001)-(1\times 4)$ surface.

II. EXPERIMENTS

All TPD experiments were carried out in an ultra-high vacuum (UHV) system with a base pressure below 2×10^{-10} mbar. The desorption products were detected by a quadrupole mass spectrometer (QMS, MAX-120, Extrel) in the chamber, equipped with an Ar ion gun (ISE 5, Omicron) for sample treatment and a low-energy electron diffraction and Auger electron spectrometer (LEED/AES, SPECTALEED, Omicron) for analysis of surface elements and structure. The preparation of the anatase $\text{TiO}_2(001)-(1\times 4)$ single crystal film was accomplished in another UHV multifunctional apparatus, consisting of a pulsed laser deposition (PLD) chamber (pressure of 1×10^{-10} mbar), a scanning tunneling microscopy (STM) chamber (3×10^{-11} mbar, Omicron) and an X-ray/ultraviolet photoemission spectroscopy (XPS/UPS) analysis chamber (8×10^{-11} mbar, VG Scienta). The anatase $\text{TiO}_2(001)$ sample was grown by means of PLD on a 0.7 wt% Nb-doped $\text{SrTiO}_3(001)$ substrate, which was in O_2 atmosphere with pressure of 1.5×10^{-5} mbar at 920 K during deposition. Details of the process of film growth have previously been described elsewhere [34, 36]. The as-grown surface was

* Authors to whom correspondence should be addressed. E-mail: xfcui@ustc.edu.cn, bwang@ustc.edu.cn; Tel.: +86-551-63602955

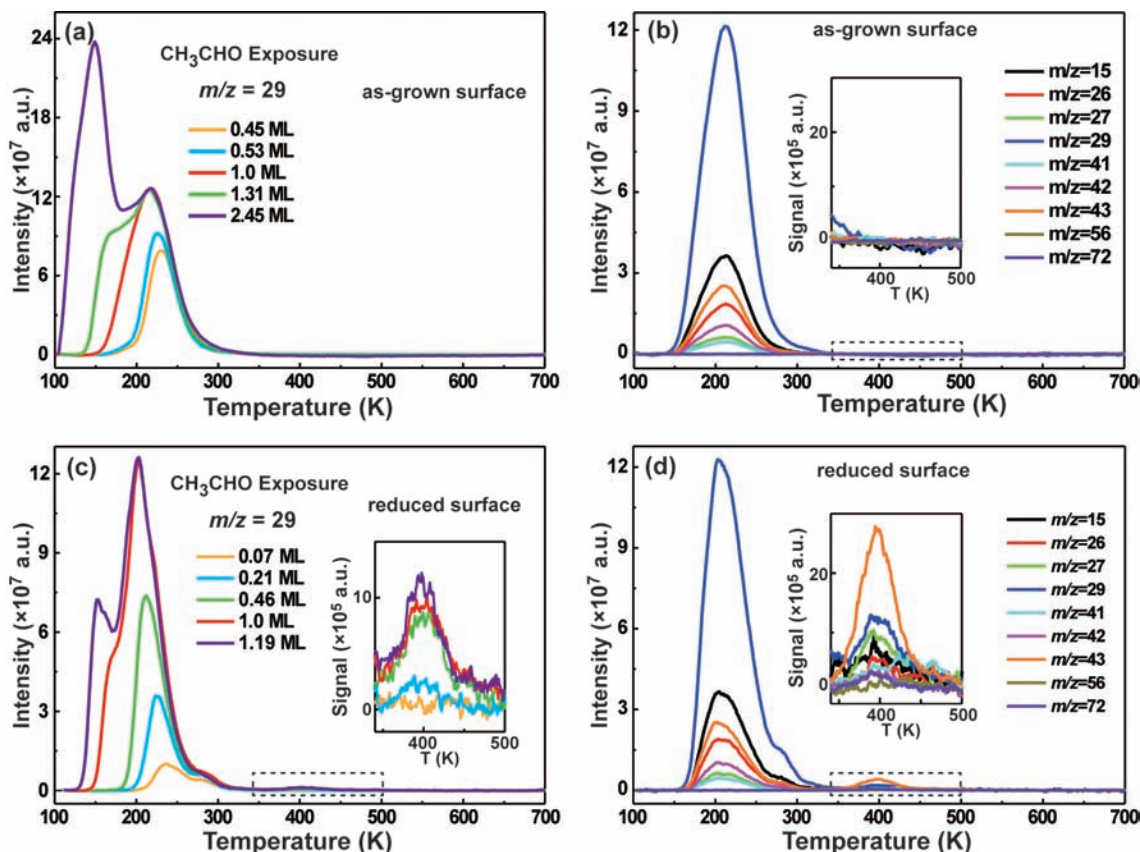


FIG. 1 (a) TPD spectra of $m/z=29$ (CHO^+) collected at various coverages of CH_3CHO on the as-grown surface. (b) TPD spectra of $m/z=15$ (CH_3^+), 26 (C_2H_2^+), 27 (C_2H_3^+), 29 (CHO^+), 41 (C_2HO^+ and/or C_3H_5^+), 42 ($\text{C}_2\text{H}_2\text{O}^+$ and/or C_3H_6^+), 43 ($\text{C}_2\text{H}_3\text{O}^+$ and/or C_3H_7^+), 56 (C_4H_8^+), and 72 ($\text{C}_4\text{H}_8\text{O}^+$) at the CH_3CHO coverage of 1.0 ML. (c) TPD spectra of $m/z=29$ (CHO^+) collected at various coverages of CH_3CHO on the reduced surface, (d) TPD spectra of $m/z=15$ (CH_3^+), 26 (C_2H_2^+), 27 (C_2H_3^+), 29 (CHO^+), 41 (C_2HO^+ and/or C_3H_5^+), 42 ($\text{C}_2\text{H}_2\text{O}^+$ and/or C_3H_6^+), 43 ($\text{C}_2\text{H}_3\text{O}^+$ and/or C_3H_7^+), 56 (C_4H_8^+) and 72 ($\text{C}_4\text{H}_8\text{O}^+$) at the CH_3CHO coverage of 1.0 ML. The insets in (b), (c) and (d) show the enlarged signals in the range of 340–500 K.

transferred to TPD chamber under the protection of N_2 and, for the resistive heating, was adhered to a Ta foil using high temperature ceramic adhesive (552, Aremco). A K-type thermal couple was glued on the sample surface to measure the temperature. The reduced surface was obtained by 1 keV Ar ion sputtering for 3 min and annealing in vacuum at 900 K for 20 min.

Acetaldehyde (Sigma-Aldrich, 99.5%) was purified by several cycles of “freeze-pump-thaw” process and then exposed to the sample at 100 K through a home-built doser, which was composed of a leak valve to control the gas flow and a tube of 4 mm in diameter to guide the gas to the surface. TPD spectra were measured at a fixedly ramping rate of 1 K/s with the sample directly facing the QMS.

III. RESULTS AND DISCUSSION

FIG. 1(a) shows a series of TPD spectra of the mass-to-charge ratio $m/z=29$ (CHO^+) at various coverages exposures of CH_3CHO on the as-grown anatase

$\text{TiO}_2(001)-(1\times 4)$ surface, in which the surface is fully oxidized [34]. During the dosing of CH_3CHO the substrate temperature was kept at 100 K. In the spectra, the red one is defined as 1 monolayer (ML, $1 \text{ ML} = 1.73 \times 10^{-14} \text{ cm}^{-2}$, with respect to the (1×4) unit cell), in which a nearly symmetric peak locates centered at about 210 K, and the 210 K adsorption state saturated while the shoulder peak from the adsorption of second layer was about to arise. The labeled coverages are obtained by integrating the area of each spectrum, with respect to the area of the defined spectrum of 1 ML. The features in the TPD spectra for CH_3CHO are similar to the ones for CH_2O [26], but a saturated desorption peak of the first layer (at 210 K) is observed for CH_3CHO , different from the coverage-dependent signal for CH_2O . FIG. 1(b) shows the TPD spectra of simultaneously recorded signals of 1 ML CH_3CHO , in which only the signals from the molecular CH_3CHO are observed. The results indicate that the as-grown surface, that is, the fully oxidized surface, is inert for the reaction of CH_3CHO , which is consistent with the results of

methanol [29].

FIG. 1 (c) and (d) shows the results from the reduced anatase TiO₂(001)-(1×4) surface. While the desorption of molecular CH₃CHO is observed at the low temperature range, similar to the as-grown surface, an additional peak centered at 400 K is observed. The various m/z signals of the surface with 1.0 ML CH₃CHO are enlarged in the inset, which shows quite different relative intensities from the molecular CH₃CHO.

In previous studies, it was reported that the aldol condensation of CH₃CHO to produce crotonaldehyde and crotyl alcohol occurs on the oxidized rutile TiO₂(001) surface [12, 13], whereas the reductive coupling to produce butene occurs on the reduced rutile TiO₂(001) surface [14]. In the most studied rutile TiO₂(110) surface, the products of butene on reduced surface and acetate on oxidized surface [15] were also observed with the desorption of molecular CH₃CHO at low temperature range. In a recent work by Yang's group, the important role of the bridging-bonded oxygen vacancies to produce 2-butanone and butene has been reported [11]. While most investigations of CH₃CHO adsorption on TiO₂ surfaces were based on rutile phase, only a small amount of experimental work was performed for aldehyde on anatase TiO₂ surfaces [16, 26]. Recently, TPD results of CH₃CHO on the anatase TiO₂(101) surface revealed that three main reaction products, 2-butanone, crotonaldehyde and crotyl alcohol, were observed without UV illumination, and the synthesis of 2-butanone via the coupling of CH₃CHO can be improved under UV light irradiation [16]. The anatase TiO₂ (001) surface was theoretically predicted to be more reactive than rutile surfaces [37–39], the mechanism of the C–C coupling reaction is far from well understood.

To identify the products for the observed peak at around 400 K, FIG. 2 shows the observable signals of $m/z=26$ (C₂H₂⁺), 27 (C₂H₃⁺), 29 (CHO⁺), 41 (C₃H₅⁺), 42 (C₂H₂O⁺ and/or C₃H₆⁺), 43 (C₂H₃O⁺ and/or C₃H₇⁺), 56 (C₄H₈⁺), 57 (C₃H₅O⁺ and/or C₄H₉⁺) and 72 (C₄H₈O⁺) at 1.0 ML coverage of CH₃CHO on reduced surface, exposed at 100 K. There are two obvious desorption peaks centered at 390 and 430 K, as marked by the dashed lines. The desorption peaks centered at 390 K include the fragments of $m/z=26$, 27, 29, 42, 43, 57, and 72. The silence of the signal $m/z=31$ suggested that the desorption products are not crotyl alcohol or other alcohols [11]. Meanwhile, the signal of $m/z=70$ was not detected, which may exclude the possible product of crotonaldehyde through aldol condensation of CH₃CHO [12–14]. According to the NIST Chemistry WebBook [40], the product at 390 K can be assigned to the product of 2-butanone, which is similar to the reported product through a carbon-carbon coupling reaction on rutile TiO₂(110) surfaces [11] and anatase TiO₂(101) surfaces [16]. The peaks centered at 430 K include the tiny contributions from fragments of $m/z=39$, 41, and 56, which can be

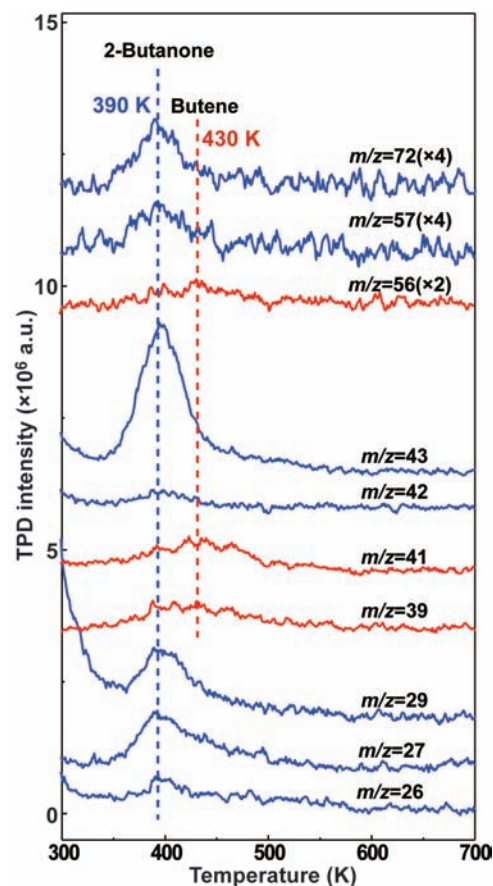


FIG. 2 TPD spectra of $m/z=26$ (C₂H₂⁺), 27 (C₂H₃⁺), 29 (CHO⁺), 39 (C₃H₃⁺), 41 (C₂HO⁺ and/or C₃H₅⁺), 42 (C₂H₂O⁺ and/or C₃H₆⁺), 43 (C₂H₃O⁺ and/or C₃H₇⁺), 56 (C₄H₈⁺), 57 (C₃H₅O⁺ and/or C₄H₉⁺) and 72 (C₄H₈O⁺) at the coverage of 1.0 ML CH₃CHO on reduced surface, exposed at 100 K. The desorption peaks at 390 and 430 K are marked by the blue and red dashed lines.

assigned to the product of butene [41]. The product of butene was also observed in the C–C coupling reaction of acetaldehyde on other surfaces [11, 12], which are ascribed to the reductive coupling of CH₃CHO adsorbed at the defects of the reduced surface. Our results show that both products of 2-butanone and butene can be produced through the thermally driven reactions of CH₃CHO at the defect sites of the reduced anatase TiO₂(001)-(1×4) surface.

FIG. 3 shows the dependence of signals ($m/z=43$ and 39) on the CH₃CHO coverages and the different substrate treatments. It can be seen that the productions of 2-butanone and butene tend to be saturated when the CH₃CHO coverages are higher than about 0.5 ML, as shown in the insets of FIG. 3 (a) and (c). The saturation of the signals can be associated with the number of the specific active sites that the coupling reactions of CH₃CHO take place. In comparison, there is no detectable product from the coupling reactions on the as-grown surface. Therefore, we conclude that the re-

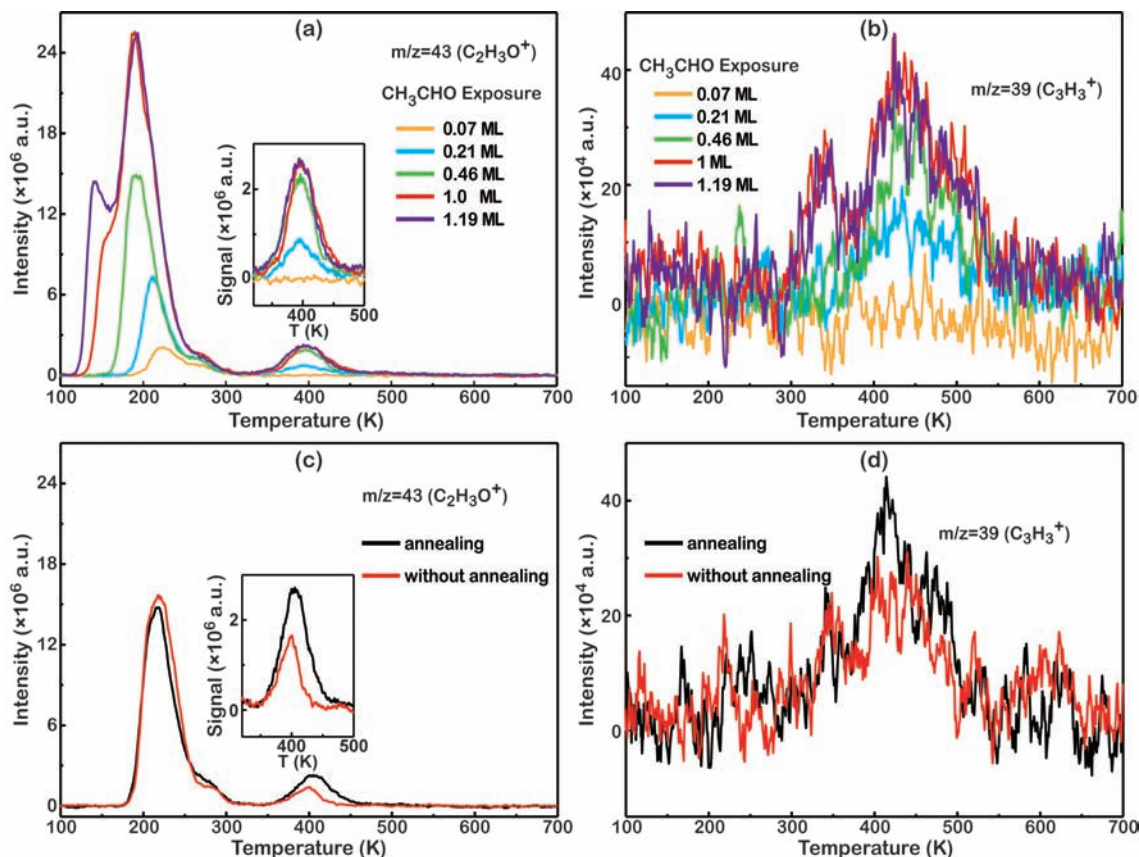


FIG. 3 TPD spectra of (a) $m/z=43$ ($C_2H_3O^+$) and (b) $m/z=39$ ($C_3H_3^+$) obtained at various CH_3CHO coverages on the reduced anatase $TiO_2(001)-(1\times 4)$ surface. (c) $m/z=43$ ($C_2H_3O^+$) and (d) $m/z=39$ ($C_3H_3^+$) obtained after different substrate treatments, for the CH_3CHO coverage of 0.5 ML. The CH_3CHO molecules were exposed at 100 K. After about tens of cycles, the production of 2-butanone and butene occurring at 400 K tends to decrease (red lines in (c) and (d), without annealing to a high temperature of 850 K), but can be recovered after annealing to 850 K for 20 min (black lines in (c) and (d)). The insets in (a) and (c) correspond to the amplified signal of $m/z=43$ from 320 K to 500 K.

duced defects, that is, the reduced Ti-pair sites [34], can be the active sites for the coupling reactions, which is similar to the reactions of formaldehyde and methanol at the reduced defects of the anatase $TiO_2(001)-(1\times 4)$ surface [26, 29, 30]. In our experiment, the concentration of the reduced defect sites is about 0.02–0.03 ML. According to the ionization cross sections of CH_3CHO [42] and 2-butanone [43] and the areas of $m/z=29$ at the CH_3CHO coverage of 1 ML in FIG. 1(c), we obtain that the production of 2-butanone is about 0.017 ML, well corresponding to the concentration of the reduced defect sites. Due to the tiny amount of butene and the less pronounced peak at 430 K, such an estimation for butene is not available, but it can be just seen that butene is a byproduct in comparison with the 2-butanone.

We also observed that after repeating measurements up to tens of cycles, the productions of 2-butanone and butene tend to decrease, as shown by the red lines in the TPD spectra in FIG. 3 (c) and (d). Note that in the TPD measurements, the samples were only heated to 700 K. We find that the decreased productions of 2-

butanone and butene can be recovered after having the sample annealed at 850 K for 20 min.

On the basis of our observations, we suggest that the C–C coupling reactions of acetaldehyde should take place at the reduced defect sites. FIG. 4 shows the schematic drawing of the reaction routes to produce 2-butanone and butene. According to the identified reduced defect sites, there are a pair of four-fold coordinate Ti (Ti_{4c}) atoms in the (1×4) ridges [34], at which the adsorbed CH_3CHO pair should be responsible for the C–C coupling reaction (FIG. 4(a)). After the desorption of 2-butanone at 390 K (FIG. 4(b)) or the desorption of butene at 430 K (FIG. 4(c)), one O atom or two O atoms may be left on the surface and partially oxidize the Ti_{4c} defect. This may explain the reduction of the activity of the surface after cycles of measurements. The procedure by annealing treatment of the surface up to 850 K for 20 min in UHV can lead to the desorption of the additional O atoms [34], and recover the reduction of the surface. In the route of butene production, leaving two O atoms should be less favored, leading to the formation of butene as a byproduct.

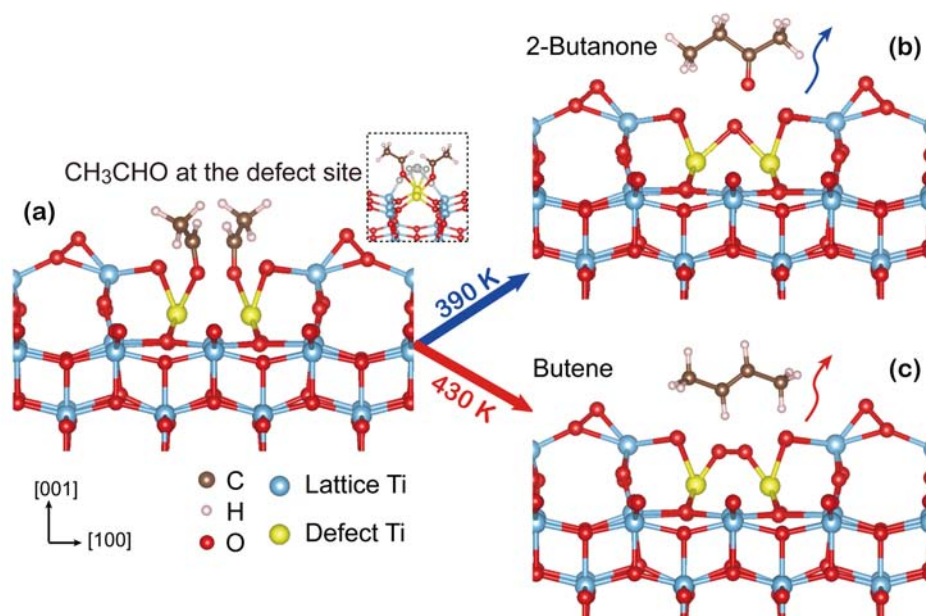


FIG. 4 Schematic drawings of (a) adsorption of paired CH₃CHO at the reduced Ti_{4c} pair, (b) production of 2-butanone by leaving one O atom at the defect site, and (c) production of butene by leaving two O atoms at the defect site. The inset shows the side view of (a).

IV. CONCLUSION

In this work, we have conducted TPD experiments to study the chemistry of CH₃CHO on the anatase TiO₂(001) surface. The experimental results demonstrate that the perfect lattice sites of the surface are quite inert for the reaction of CH₃CHO, while the reduced defect sites are active for the C–C coupling reactions of CH₃CHO to form 2-butanone and butene products on the surface. Our findings provide an insightful understanding for the coupling reactions of CH₃CHO on the reduced anatase TiO₂(001) surface.

V. ACKNOWLEDGMENTS

This work was supported by the Ministry of Science and Technology of China (No.2016YFA0200603), the National Natural Science Foundation of China (No.91421313 and No.21573207), and Anhui Initiative in Quantum Information Technologies (AHY090300).

- [1] G. W. Huber, S. Iborra, and A. Corma, *Chem. Rev.* **106**, 4044 (2006).
- [2] V. L. Sushkevich, I. I. Ivanova, V. V. Ordonsky, and E. Taarning, *ChemSusChem* **7**, 2527 (2014).
- [3] C. C. C. Johansson Seechurn, M. O. Kitching, T. J. Colacot, and V. Snieckus, *Angew. Chem. Int. Ed.* **51**, 5062 (2012).

- [4] A. Gumidyala, B. Wang, and S. Crossley, *Sci. Adv.* **2**, e1601072 (2016).
- [5] L. X. Yin and J. Liebscher, *Chem. Rev.* **107**, 133 (2007).
- [6] U. Diebold, *Surf. Sci. Rep.* **48**, 53 (2003).
- [7] L. C. Pang, R. Lindsay, and G. Thornton, *Chem. Soc. Rev.* **37**, 2328 (2008).
- [8] A. Fujishima, X. Zhang, and D. A. Tryk, *Surf. Sci. Rep.* **63**, 515 (2008).
- [9] M. A. Henderson, *Surf. Sci. Rep.* **66**, 185 (2011).
- [10] Y. Wang, A. A. Liu, D. G. Ma, S. H. Li, C. C. Lu, T. Li, and C. C. Chen, *Catalysts* **8**, 355 (2018).
- [11] W. S. Yang, Z. H. Geng, C. B. Xu, Q. Guo, D. X. Dai, and X. M. Yang, *J. Phys. Chem. C* **118**, 27920 (2014).
- [12] H. Idriss, K. Pierce, and M. A. Barteau, *J. Am. Chem. Soc.* **113**, 715 (1991).
- [13] H. Idriss, K. S. Kim, and M. A. Barteau, *J. Catal.* **139**, 119 (1993).
- [14] H. Idriss and M. A. Barteau, *Catal. Lett.* **40**, 147 (1996).
- [15] R. T. Zehr and M. A. Henderson, *Surf. Sci.* **602**, 2238 (2008).
- [16] Z. H. Geng, X. Chen, W. S. Yang, Q. Guo, D. X. Dai, and X. M. Yang, *J. Phys. Chem. C* **120**, 9897 (2016).
- [17] J. E. Rekoske and M. A. Barteau, *Langmuir* **15**, 2061 (1999).
- [18] S. C. Luo and J. L. Falconer, *Catal. Lett.* **57**, 89 (1999).
- [19] M. Singh, N. J. Zhou, D. K. Paul, and K. J. Klabunde, *J. Catal.* **260**, 371 (2008).
- [20] L. Benz, J. Haubrich, R. G. Quiller, and C. M. Friend, *Surf. Sci.* **603**, 1010 (2009).
- [21] L. Benz, J. Haubrich, R. G. Quiller, S. C. Jensen, and C. M. Friend, *J. Am. Chem. Soc.* **131**, 15026 (2009).
- [22] H. Idriss, K. G. Pierce, and M. A. Barteau, *J. Am. Chem. Soc.* **116**, 3063 (1994).
- [23] J. J. Plata, V. Collico, A. M. Mrquez, and J. F. Sanz,

- J. Phys. Chem. C **115**, 2819 (2011).
- [24] M. J. Yao, Y. M. Ji, H. H. Wang, Z. M. Ao, G. Y. Li, and T. C. An, J. Phys. Chem. C **121**, 13717 (2017).
- [25] C. B. Xu, W. S. Yang, Q. Guo, D. X. Dai, M. D. Chen, and X. M. Yang, J. Am. Chem. Soc. **135**, 10206 (2013).
- [26] B. Luo, H. Q. Tang, Z. W. Cheng, Y. Y. Ji, X. F. Cui, Y. L. Shi, and B. Wang, J. Phys. Chem. C **121**, 17289 (2017).
- [27] A. M. Nadeem, J. M. Muir, K. A. Connelly, B. T. Adamson, B. J. Metson, and H. Idriss, Phys. Chem. Chem. Phys. **13**, 7637 (2011).
- [28] F. P. Rotzinger, J. M. Kesselman-Truttmann, S. J. Hug, V. Shklover, and M. Grätzel, J. Phys. Chem. B **108**, 5004 (2004).
- [29] H. Q. Tang, Z. W. Cheng, S. H. Dong, X. F. Cui, H. Feng, X. C. Ma, B. Luo, A. D. Zhao, J. Zhao, and B. Wang, J. Phys. Chem. C **121**, 1272 (2017).
- [30] Z. W. Cheng, H. Q. Tang, X. F. Cui, S. H. Dong, X. C. Ma, B. Luo, S. J. Tan, and B. Wang, J. Phys. Chem. C **121**, 19930 (2017).
- [31] S. J. Tan and B. Wang, Chin. J. Chem. Phys. **28**, 383 (2015).
- [32] Z. H. Geng, X. Chen, Q. Guo, D. X. Dai, and X. M. Yang, Chin. J. Chem. Phys. **30**, 1 (2017).
- [33] X. Chen, F. L. Li, Q. Guo, D. X. Dai, and X. M. Yang, Chin. J. Chem. Phys. **31**, 547 (2018).
- [34] Y. Wang, H. J. Sun, S. J. Tan, H. Feng, Z. W. Cheng, J. Zhao, A. D. Zhao, B. Wang, Y. Luo, J. L. Yang, and J. G. Hou, Nat. Commun. **4**, 2214 (2013).
- [35] H. J. Sun and J. Zhao, J. Phys. Chem. C **122**, 14528 (2018).
- [36] H. Q. Tang, Y. Lin, Z. W. Cheng, X. F. Cui, and B. Wang, Chin. J. Chem. Phys. **31**, 71 (2018).
- [37] X. Q. Gong and A. Selloni, J. Phys. Chem. B **109**, 19560 (2005).
- [38] X. Q. Gong, A. Selloni, and A. Vittadini, J. Phys. Chem. B **110**, 2804 (2006).
- [39] A. Vittadini, M. Casarin, and A. Selloni, Theor. Chem. Acc. **117**, 663 (2006).
- [40] <https://webbook.nist.gov/cgi/cbook.cgi?ID=C78933&Units=SI&Mask=200>
- [41] <https://webbook.nist.gov/cgi/cbook.cgi?ID=C624646&Units=SI&Mask=200>
- [42] J. R. Vacher, F. Jorand, N. Blin-Simiand, and S. Pasquiers, Chem. Phys. **323**, 587 (2006).
- [43] J. R. Vacher, F. Jorand, N. Blin-Simiand, and S. Pasquiers, Int. J. Mass spectrom. **273**, 117 (2008).